



Organized Intrafibrillar Mineralization, Directed by a Rationally Designed Multi-Functional Protein

Journal:	<i>Journal of Materials Chemistry B</i>
Manuscript ID:	TB-ART-02-2015-000386.R2
Article Type:	Paper
Date Submitted by the Author:	21-Apr-2015
Complete List of Authors:	<p>Ping, Hang; State Key Laboratory of Advanced Technology for Materials Synthesis and Processing, Xie, Hao; Wuhan University of Technology, School of Chemistry, Chemical Engineering, and Life Science Su, Bao-Lian; University of Namur, Laboratory of Inorganic Materials Chemistry (CMI)/Research Centre for nanomaterials Chemistry (CNANO) Cheng, Yi-Bing; Monash University, Materials Engineering Wang, Weimin; Wuhan University of Technology, The State Key Laboratory of Advanced Technology for Materials Synthesis and Processing Wang, Hao; Wuhan University of Technology, The State Key Laboratory of Advanced Technology for Materials Synthesis and Processing Wang, Yucheng; Wuhan University of Technology, The State Key Laboratory of Advanced Technology for Materials Synthesis and Processing Zhang, Jinyong; Wuhan University of Technology, State Key Laboratory of Advanced Technology for Materials Synthesis and Processing Zhang, Fan; Wuhan University of Technology, State Key Laboratory of Advanced Technology for Materials Synthesis and Processing Fu, Zhengyi; Wuhan University of Technology, The State Key Laboratory of Advanced Technology for Materials Synthesis and Processing</p>

PAPER

Organized Intrafibrillar Mineralization, Directed by a Rationally Designed Multi-Functional Protein

Cite this: DOI: 10.1039/x0xx00000x

Hang Ping,^a Hao Xie,^{b†} Bao-Lian Su,^c Yi-bing Cheng,^d Weimin Wang,^a Hao Wang,^a Yucheng Wang,^a Jinyong Zhang,^a Fan Zhang^a and Zhengyi Fu^{a†}

Received 00th January 2012,
Accepted 00th January 2012

DOI: 10.1039/x0xx00000x

www.rsc.org/

Taking lessons from the structure-forming process of biominerals in animals and plants, one can find tremendous inspirations and ideas for developing advanced synthesis techniques. Bone, as a typical representative of biominerals, is constituted of mineralized collagen fibrils, which are formed under the functions of non-collagenous proteins (NCPs). Intrafibrillar mineralization is the consequence of a synergy among several NCPs. In the present study, we have designed a multi-functional protein, named (MBP)-BSP-HAP, based on bone sialoprotein (BSP) and hydroxyapatite binding protein (HAP), to mimic the intrafibrillar mineralization process *in vitro*. The three functional domains of (MBP)-BSP-HAP provide the artificial protein with multiple designated functions for intrafibrillar mineralization including binding calcium ions, binding collagen, and binding hydroxyapatite. Platelet-like hydroxyapatite crystals periodically arranged inside the collagen fibrils have been achieved under the function of (MBP)-BSP-HAP. The mechanism of intrafibrillar mineralization directed by the multi-functional protein was proposed. This work may not only shed light on bio-process inspired approaches for more economic and efficient biomimetic synthesis, but also be helpful in understanding the natural process of bone formation for bone regeneration and tissue repair.

Introduction

Biominerals in nature (e.g. bones, shells and teeth) resulting from many billions of years of evolution, possess exquisite hierarchical and organic-inorganic composite structures, which determine their outstanding mechanical behavior and adaptability.^{1,2} In recent decades, a lot of research has been focused on learning the unique structures of biominerals in order to obtain superior properties in new materials.^{3,4} Inspired by the structural and functional integrity of biominerals, scientists have created “bio-inspired materials”³⁻⁵ or “bio-inspired functions”.^{6,7} Moreover, the elaborate biological process to form biominerals is astonishing and fascinating. A good example is the formation of calcite spicules, whose final, smoothly curved fibrous morphology is assembled via amorphous calcium carbonate particles at an initial stage due to the self-assembly property of silicatein- α . In this way, the high protein content and slippery fiber surfaces are responsible for the extreme bending strength and light-guiding function.^{8,9} In the biomineralization process, specialized biomineralization-related proteins, combining unique characteristics of sequence-specific self-assembly¹⁰ and biomineral recognition,¹¹ play vital roles in directing the formation of complex and hierarchical composite structures.¹² Taking lessons from the structure-forming process of biominerals, one can find tremendous inspiration and ideas for developing advanced synthesis techniques, which may be called bio-process inspired synthesis.

Bone is a typical representative of biominerals and has been intensively investigated due to its integration combinations of complex structure and outstanding mechanical properties.¹³⁻¹⁵ The elementary building blocks of bone are the mineralized collagen fibrils, which contain nanoapatite crystals uniaxially oriented inside the fibril.¹⁶ The intricate hierarchical structure, though assembled from weak components, collagen and hydroxyapatite, is responsible for the excellent performance of bone.^{5,17} Moreover, the process of bone formation is complicated and involves a lot of proteins. During the process of bone formation, it is believed that acidic non-collagenous proteins (NCPs) initially produce and stabilize amorphous calcium phosphate phase, and then regulate the infiltration of calcium phosphate into collagen fibrils.^{18,19} It has been shown that the charged surface or functional domains of some proteins, such as osteocalcin¹¹ and antifreeze protein,^{20,21} can recognize crystal lattice and also control the crystal nucleation and growth *in vitro*. However, the details of the collagen fibril mineralization mechanism remain unclear.²² Intrafibrillar mineralization is the consequence of synergy several NCPs. Over the last few years, numerous studies have focused on the mineralization of reconstituted collagen fibril, thereby comprehending the process of mineral deposition and orientation *in vitro*,²³ because the minerals inside collagen fibrils are the basic and significant factor for mimicking natural bone formation. Intrafibrillar mineralization has been successfully achieved by using polyacrylic acid¹⁸ or polyaspartic acid^{24,25} as a biomimetic analogue. A polymer-

induced liquid precursor (PILP) process has been proposed to explain these phenomena, since the highly hydrated and fluidic character of PILP droplets enable the drops to be drawn into fibrils by capillary action.^{18,26,27} Phosphorylated dentin matrix protein 1 (DMP) and dentin phosphophoryn (DPP), both NCPs,²⁸ have also been used, respectively, to regulate the formation of mineralized fibrils. Nevertheless, neither a single NCP nor an analogue alone possesses all features of other NCPs, and it lacks the potential of templating mineral deposition inside fibrils.²⁹ Recently, by adopting a strategy of dual analogues, with the combination of polyacrylic acid as sequestration analogue and inorganic polyphosphates as templating analogue, intrafibrillar mineralization has been achieved via hierarchical nanoapatite assembly.²⁹⁻³¹ So far, the work has been mainly focused on the using of polymers or single protein from NCPs to induce the collagen intrafibrillar mineralization. Limited work was reported using recombinant proteins mimicking bone proteins, which have functions to direct the mineralization.

In the present study, we designed a multi-functional protein, called BSP-HAP, based on bone sialoprotein (BSP) and hydroxyapatite binding peptide (HAP), to simulate the intrafibrillar mineralization process *in vitro* to reveal the mechanism of collagen fibril mineralization. BSP is the most abundant NCP in bone, constituting approximately 15 wt% of the total NCPs,³² and it plays a crucial role in bone formation. BSP with an open and flexible conformation in solution, has two acidic domains rich in glutamic and aspartic acid residues providing calcium ions binding sites.¹⁹ BSP can also bind to collagen via hydrophobic interaction, and BSP-collagen has a co-operative effect in mineral formation.³³ On the other hand, HAP is a strong hydroxyapatite-binding peptide, which is proposed to take advantages of short peptides to interact with minerals.³⁴ With the development of genetically engineered peptides for inorganic solids (GEPIS),³⁵ lots of oligopeptides have been identified and utilized in material synthesis.^{12,36} HAP can be obtained through phage display.³⁷ Therefore, the BSP-HAP shows three domains with multiple functions: binding calcium ions, binding collagen and binding hydroxyapatite, which are expected to work together to direct the collagen intrafibrillar mineralization.

Experimental

Expression and purification of recombinant protein

The coding sequence of human bone sialoprotein (BSP) and hydroxyapatite binding peptides (HAP) were synthesized and cloned into the pMAL-c4x vector (New England Biolabs, USA) downstream of the maleE gene (Fig. 1a). The resulting plasmid is pMAL(BSP-HAP) (Fig. 1b), encoding the gene of protein (MBP)-BSP-HAP (Fig. S1). All constructs were confirmed by restriction enzyme digestion and DNA sequencing. Expression and purification of (MBP)-BSP-HAP was based on pMAL Protein Fusion & Purification System User Manual (New England Biolabs, USA). A single colony of *E. coli* BL21 (DE3) harboring pMAL(BSP-HAP) was injected into Luria-Bertani (LB) medium containing 100 $\mu\text{g ml}^{-1}$ ampicillin and shaking at 37 °C overnight. The cell suspension was injected into LB medium, followed by shaking at 37 °C until an OD₆₀₀ of 0.5-0.6 was reached. Protein expression was initiated by supplying 1 mM of isopropyl-p-D-thiogalactoside (IPTG) and continued shaking at 37 °C for 3 h. Cells were harvested by centrifugation at 6,000 g and 4 °C, and then re-suspended in buffer A (50 mM Tris(hydroxymethyl)aminomethane hydrochloride (Tris-HCl),

pH 8.5; 100 mM NaCl), and lysed by a French press. The cell lysate was centrifuged at 10,000 g for 30 min to remove cell debris and applied to amylose affinity resin, which was washed and pre-equilibrated with buffer A. Unbound proteins were washed with buffer A. The bound (MBP)-BSP-HAP was eluted with buffer A containing 20 mM maltose and dialyzed against buffer A.

Assembly of collagen fibrils

Collagen stock solution was prepared by dissolving lyophilized type I collagen powder (Sigma-Aldrich, USA) in 0.1 M acetic acid at 4 °C overnight. Then 30 μl aliquot of collagen stock solution was deposited over poly(lysine)-coated glass coverslips and reconstitution was initiated by neutralizing the collagen stock solution with ammonia vapor in a humidity chamber for 3 h. Subsequently, the ammonium hydroxide solution was removed and the collagen solution was incubated at room temperature for 21 h.

Biological activity characterization of multi-functional protein

The binding activity of the multi-functional protein to calcium was tested by calcium ion absorption assay. MBP or (MBP)-BSP-HAP were loaded on amylose resin (protein final concentration was 0.1 mg ml⁻¹) and mixed with 10 mM N-(2-Hydroxyethyl)piperazine-N'-(2-ethanesulfonic acid) (HEPES), pH=7.4, 5 mM CaCl₂ (Sinopharm, China), followed by gently shaking for four hours. Amylose resin did not bind calcium ions (Fig. S2). The mixtures were collected at 2 h intervals and the resin was removed by centrifugation. The calcium ions remaining in the supernatant were examined by inductively coupled plasma atomic emission spectroscopy (ICP-AES, PerkinElmer, Optima 4300DV).

The binding activity of multi-functional protein to collagen or hydroxyapatite was tested by fluorescein isothiocyanate isomer I (FITC, Sangon Biotech, China)-labeled fluorescence technology. The multi-functional protein (1 mg ml⁻¹) was dialyzed three times against a solution containing 90 mM NaHCO₃, 10 mM Na₂CO₃, 120 mM NaCl (Sinopharm, China). Then FITC was slowly added into protein solution to reach a final concentration of 0.15 mg ml⁻¹. The mixture was shaken on an agitator for 8 h, and then filtered and dialyzed against distilled water for 24 h at 4 °C. FITC-labeled (MBP)-BSP-HAP was incubated overnight on glass coverslips with hydroxyapatite powder (Aladdin, China) or collagen fibrils. After washing three times with deionized water, the samples were air dried and imaged by fluorescent microscopy (Olympus, IX71).

Mineralization of collagen fibrils

HEPES buffer (10 mM, pH=7.4) containing 2.7 mM CaCl₂ and 1.35 mM K₂HPO₄ (Sinopharm, China) was used as the mineral solution. For the control samples, the glass coverslip coated with collagen fibrils was incubated in HEPES buffer alone and kept at 37 °C for several days. In the presence of additives, collagen mineralization was achieved by incubating the collagen-coated coverslip in HEPES buffer containing 100 $\mu\text{g ml}^{-1}$ polyacrylic acid (Alfa-Aesar, USA) and/or 2 $\mu\text{g ml}^{-1}$ multi-functional protein (MBP)-BSP-HAP.

Field emission scanning electron microscopy (FESEM)

The mineralized samples were morphological characterized through field emission scanning electron microscopy (FESEM,

Hitachi, S4800). The samples were placed on a carbon tape and sputter-coated with platinum prior to characterization at 10 kV.

Transmission electron microscopy (TEM)

The samples were scratched from coverslips and dispersed in alcohol through ultrasonic treatment, then transferred directly to ultrathin carbon coated copper grids. The grids were examined unstained using transmission electron microscopy (TEM, JEOL, JEM-2010F) and selected area electron diffraction techniques (SAED) at 110 kV. The fine structure of isolated collagen fibril was investigated by high resolution transmission electron microscopy (HRTEM, JEOL, JEM-2100F) at 200 kV.

Fourier transform infrared spectroscopy (FTIR)

The mineralized products scratching from coverslips were grinded with potassium bromide and then pressed into pellets. The infrared spectra of pellets were collected from 4000 to 400 cm^{-1} using fourier transform infrared spectroscopy (FTIR, ThermoScientific, Nicolet6700) with a resolution of 4 cm^{-1} using 32 scans.

Results and discussion

Design, expression and purification of recombinant protein

To facilitate the expression and purification of BSP-HAP, the maltose binding protein (MBP) was fused to the N-terminus of BSP-HAP and obtained the multi-functional protein (MBP)-BSP-HAP (Fig. 1a and 1b). Fragment MBP, an affinity tag, tighter binding to amylose resin through hydrogen bond, which can improve the solubility of recombinant protein in solution and facilitate purification. Although MBP contains acidic residues (PDB ID: 1ANF)³⁸ and may interact with calcium ions, there are no reports of MBP concerning hydroxyapatite mineralization to the best of our knowledge. In subsequent studies, MBP protein was used as control for investigating activities of (MBP)-BSP-HAP. Affinity purification of (MBP)-BSP-HAP has been achieved to 95% homogeneity (Fig. 1c). Typically, a protein yield of 10 mg L^{-1} culture medium can be expected.

The secondary structure of purified multi-functional protein (MBP)-BSP-HAP and its' fragments MBP, (MBP)-BSP, and HAP were analysed by circular dichroism (CD) spectroscopy (Fig. S3). The secondary structure of HAP was significantly different from those of other three proteins. With a ellipticity band near 200 nm^{-1} , random coil is the dominant secondary structure of HAP.³⁷ With a peak at 195 nm^{-1} and a valley near 216 nm^{-1} , beta sheet is the dominant secondary structure of MBP, (MBP)-BSP, and (MBP)-BSP-HAP.

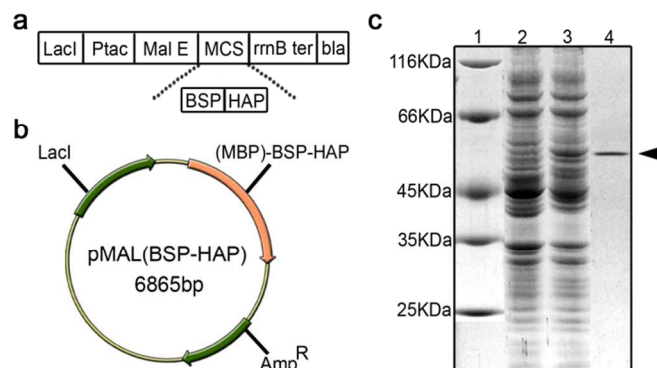


Fig. 1 Design, expression and purification of multi-functional protein. (a) The genetic elements of vector: LacI, repressor; Ptac, promoter; Mal E, gene of MBP; MCS, multiple cloning site; rmb ter, transcriptional terminator; bla, ampicillin resistance gene. (b) Scheme of plasmid vector of pMAL(BSP-HAP), encoding the multi-functional protein (MBP)-BSP-HAP. (c) Expression and purification of (MBP)-BSP-HAP, analyzed with 10% SDS-PAGE. Lane 1, molecular weight marker; lane 2, lysate of uninduced cells; lane 3, IPTG-induced cells; lane 4, affinity purified (MBP)-BSP-HAP.

Biological activity of recombinant protein

Specific interactions were observed between (MBP)-BSP-HAP and calcium ions. In contrast to MBP, (MBP)-BSP-HAP exhibits a significant ability to bind calcium ions (Fig. 2). Since the BSP fragment in (MBP)-BSP-HAP includes many clusters of acidic residues,³⁹ which can accumulate calcium ions from solution through their carboxylic groups.⁴⁰ Although MBP has acidic residues on its surface, these residues do not form clusters and have poor affinity to calcium ions.³⁸

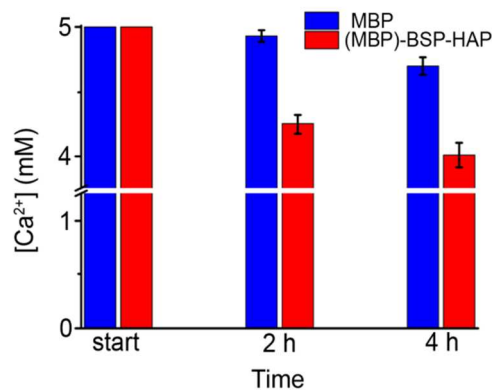


Fig. 2 The ability of binding calcium ions of proteins. Variation of calcium ion concentration in solution when calcium ions are absorbed by proteins.

By fluorescence labeling, the specific binding activity of (MBP)-BSP-HAP to hydroxyapatite and collagen fibrils has been confirmed. Upon interaction with FITC-labeled (MBP)-BSP-HAP, significantly strong fluorescence has been observed on hydroxyapatite and collagen fibrils (Fig. 3), indicating absorbance of (MBP)-BSP-HAP into these materials. Therefore, upon the activities of BSP and HAP, the two functional domains with high affinity to hydroxyapatite and collagen, (MBP)-BSP-HAP exhibits significant binding activity to hydroxyapatite and collagen. Being attached to collagen enables (MBP)-BSP-HAP to promote the formation of hydroxyapatite. However, when FITC-labeled MBP interacts with hydroxyapatite or collagen, poor fluorescence has been

evidenced (Fig. S4), indicating there are weak nonspecific interactions between MBP and these two materials.

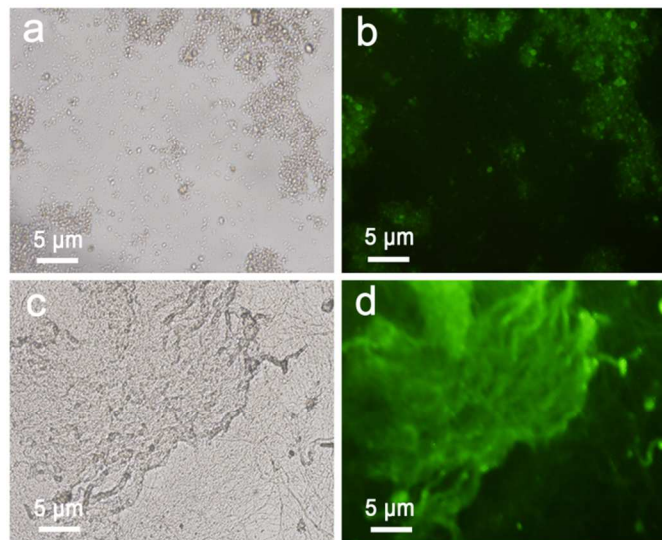


Fig. 3 The ability of binding hydroxyapatite powder and collagen fibrils of 1 mg ml^{-1} (MBP)-BSP-HAP. (a) and (c) Bright field images of hydroxyapatite powder and collagen fibrils incubated with FITC-labeled (MBP)-BSP-HAP; (b) and (d) Fluorescence images of hydroxyapatite powder and collagen fibrils incubated with FITC-labeled (MBP)-BSP-HAP.

Effect of multi-functional protein on collagen mineralization

Mineralization of hydroxyapatite inside collagen was further investigated under the control of (MBP)-BSP-HAP. Without any additive, flaky-shaped minerals grow along the surface of reconstituted collagen fibrils (Fig. 4a-b). Figure 4c shows a typical TEM image of a single fibril, the core-shell structure demonstrates that minerals deposit on the surface of fibril and no intrafibrillar mineralization occurs. SAED pattern reveals the polycrystalline nature and disorderly alignment of mineral (Fig. 4c inset). Flaky-shaped minerals peeling from the surface of fibrils under ultrasonic treatment are randomly distributed throughout the grid (Fig. 4d). Fourier transform infrared (FTIR) spectroscopy (Fig. S5a) shows the minerals are carbonated apatite. No characteristic peaks of type I collagen can be observed, indicating a large amount of apatite coated on fibrils' surfaces.

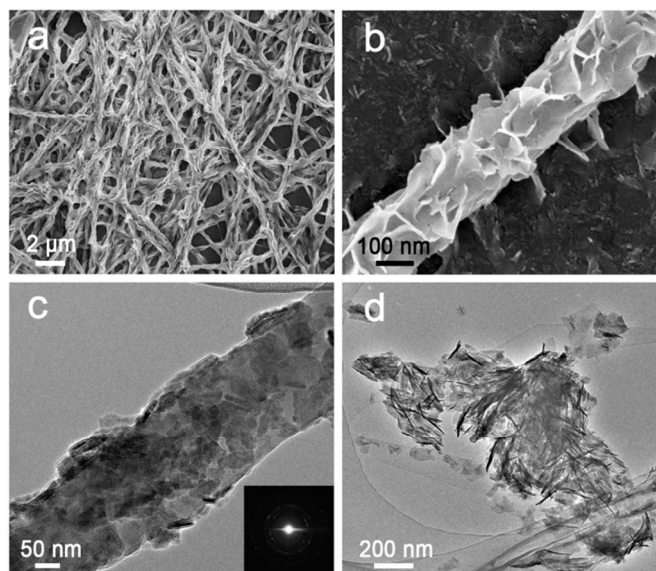


Fig. 4 Electron microscopy images of mineralized collagen fibrils without any additive for 72 h. (a) Low and (b) high magnification of SEM images of mineralized collagen fibrils, apatite crystals randomly formed along with fibril. (c) TEM image of an isolated collagen fibril (inset, SAED pattern). (d) TEM image of flaky-shaped mineral crystals.

When collagen fibrils are incubated in a mineralized solution containing polyacrylic acid, an analogue binds inorganic ions to form a liquid precursor, and the smooth surface and band pattern can be identified from mineralized fibrils (Fig. 5a-b). TEM image shows that continuous needle-like minerals grow exclusively inside fibrils, (Fig. 5c). The arc-shaped (002) diffraction plane manifests the growth orientation of minerals, paralleling to the long axis of fibril (Fig. 5d). However, similar to the control, minerals randomly distribute on the surface of collagen fibrils when only (MBP)-BSP-HAP exists in solution (Fig. S6). The effect of different fragments of (MBP)-BSP-HAP on collagen mineralization is also investigated (Fig. S7). Though BSP fragment can bind Ca^{2+} through carboxylic group, the amount of carboxylic group in BSP is far less than that of polyacrylic acid. Therefore, (MBP)-BSP-HAP and its fragments have no ability to bind inorganic ions to form a liquid precursor, and the intrafibrillar mineralization can not be achieved.

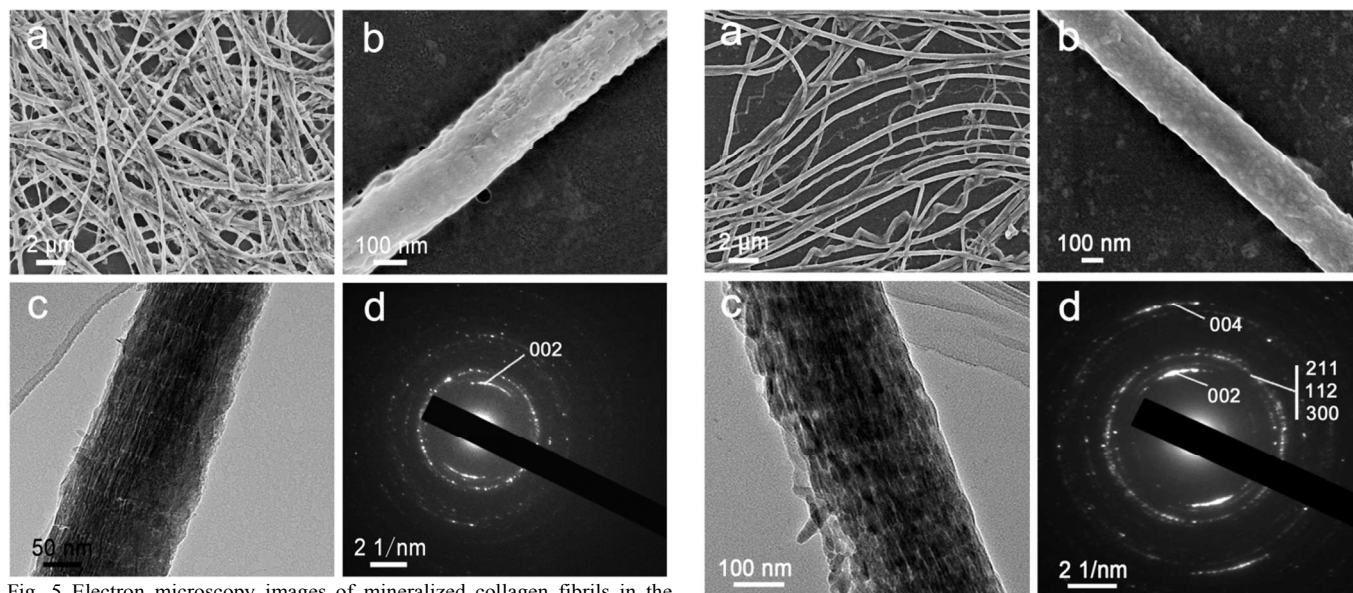


Fig. 5 Electron microscopy images of mineralized collagen fibrils in the presence of polyacrylic acid for 72 h. (a) Low and (b) high magnification of SEM images of mineralized collagen fibrils. (c) TEM image of an isolated collagen fibril, needle-like apatite crystals have grown exclusively inside fibrils. (d) SAED pattern of the mineralized fibril.

When both (MBP)-BSP-HAP and polyacrylic acid are present in a mineralization system, although fibrils' surfaces remain smooth, the obscure band pattern of collagen fibrils are observed, which can be attributed to a high degree of intrafibrillar mineralization (Fig. 6a and 6b). TEM image displays the highly organized alignment of minerals inside the fibril (Fig. 6c). The minerals are periodically arranged along the long axis of collagen fibrils. SAED pattern shows that the mineral phase inside the isolated fibril is hydroxyapatite (Fig. 6d).²⁹ The (002) and (004) planes are parallel to the long axis of the fibril. The arc-shaped pattern of the (002) and (004) diffraction planes indicates that mineral crystals are tilted, with slightly distorted orientation along their c-axis.¹⁸ On the other hand, the d-spacing of the (211), (112) and (300) diffraction planes is quite close, so the combination of these three arcs generated a continuous ring. Meanwhile, the morphology of crystals inside a fibril changes from needle to platelet. The size of crystals in the tip of a fractured fibril, is 30-50 nm in length, 15-20 nm in width (Fig. 6e). The size and shape of the hydroxyapatite crystals are similar to those of bone.⁴¹ In addition, the HRTEM image plainly reveals the growth orientation of the apatite mineral, in which the crystal lattice, with interplanar spacing of 0.34 nm, is parallel to the (002) plane of hydroxyapatite (Fig. 6f). When polyacrylic acid and different fragments of (MBP)-BSP-HAP coexist in solution, minerals with distinct morphology exclusively grow inside fibrils (Fig. S8). The needle-like minerals inside fibrils can also be observed when mixing polyacrylic acid with HAP or MBP. The morphology of minerals gradually evolves into unregular platelet, when both polyacrylic acid and (MBP)-BSP exist in mineralization system.

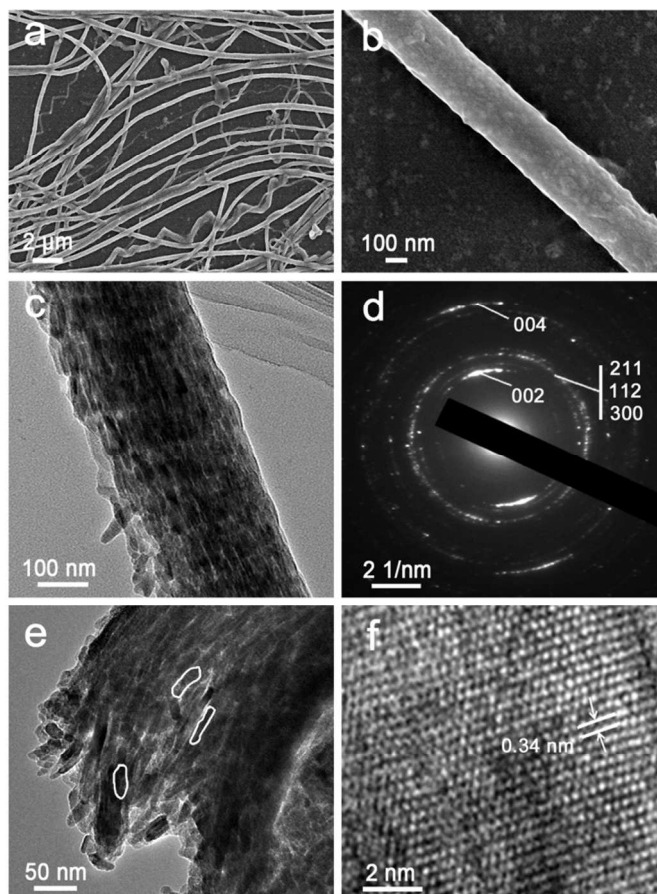


Fig. 6 Electron microscopy images of mineralized collagen fibrils and fine structure of apatite minerals inside a collagen fibril in the presence of 100 $\mu\text{g ml}^{-1}$ polyacrylic acid and 2 $\mu\text{g ml}^{-1}$ (MBP)-BSP-HAP for 72 h. (a) Low and (b) high magnification of SEM images of mineralized collagen fibrils. (c) TEM image of an isolated collagen fibril, platelet-like mineral crystals with uniform size grown inside fibril. (d) SAED pattern of the fibril, indicating that the mineral phase is apatite, and oriented parallel to the longitudinal axis of the fibril. (e) TEM image of the tip of a fractured collagen fibril, some single apatite crystals are marked by white circle. (f) An HRTEM image of apatite crystal inside fibril.

Unlike the FTIR spectra of commercially available collagen and hydroxyapatite (Fig. S5b and S5c), the characteristic peaks of collagen and hydroxyapatite are both found in our mineralized fibrils (Fig. 7). Specifically, the peaks at 1649 cm^{-1} , 1553 cm^{-1} , 1248 cm^{-1} correspond to the characteristic amide I, II and III bands of type I collagen.³¹ The peaks at 603 cm^{-1} and 563 cm^{-1} , the “fingerprints” of hydroxyapatite, are assigned to the ν_4 O-P-O bending mode.⁴² Also, the peak at 874 cm^{-1} is assigned to small amount of CO_3^{2-} substitution in the apatite lattice.¹⁷

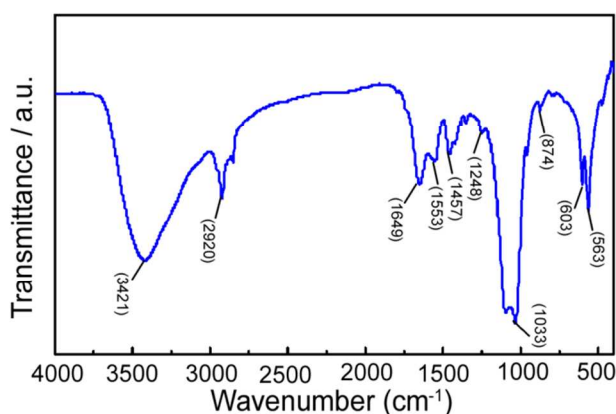


Fig. 7 FTIR spectrum of mineralized collagen fibrils in the presence of polyacrylic acid and (MBP)-BSP-HAP for 72 h.

An intrafibrillar mineralization process directed by (MBP)-BSP-HAP is proposed in Figure 8. (MBP)-BSP-HAP first specifically binds to the hole zones of collagen fibrils through hydrophobic interaction between hydrophobic residues of BSP and collagen fibrils.^{33,43} Then (MBP)-BSP-HAP can serve as a template and modulate the growth of hydroxyapatite within the hole zones. Meanwhile, polyacrylic acid acts as a cationic absorbing base, accumulating calcium ions from the solution to form droplets of amorphous calcium phosphate (ACP) in fluid phase. The negatively charged ACP is attracted to positively charged regions of the collagen fibrils through electrostatic interaction. Afterward, ACP infiltrates and diffuses throughout the interior of the collagen fibrils, owing to the highly hydrated and fluid characteristics of the amorphous phase. The (MBP)-BSP-HAP within the collagen fibrils is then surrounded by ACP. Recently, Yang et al. found that special residue sites of a nucleating motif in BSP, a peptide with a Glu-rich domain close to N-terminus, can coordinate Ca^{2+} equilateral triangle within ACP based on molecular dynamics study.⁴⁴ In addition, the size of the Ca^{2+} equilateral triangle matches the distribution of calcium atoms in the (002) plane of the hydroxyapatite crystal lattice. Our experimental studies support the notion that the BSP fragment can interact with the Ca^{2+} equilateral triangle. The transformation energy of amorphous phase changing to crystalline phase is decreased due to the size match between the Ca^{2+} equilateral triangle within ACP and the (002) plane of hydroxyapatite. So the crystals prefer to grow in alignment with the [002] axis, perpendicular to the (002) plane, and the space confinement of nearby tropocollagen molecules restrict the transverse growth of crystals. Due to the high affinity of HAP fragments to hydroxyapatite, HAP fragments can bind to mineral surfaces and restrict the growth of minerals when they reach another protein located in a neighboring hole zone. Finally, the size of platelet-like nanocrystals mentioned in Figure 6 (30–50 nm in length and 15–20 nm in width) matches well with the spacing supplied by the collagen fibril and the protein template.

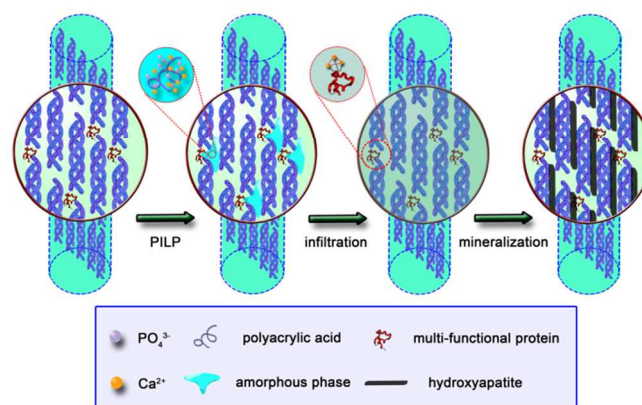


Fig. 8 Schematic of intrafibrillar mineralization process directed by (MBP)-BSP-HAP.

Conclusions

A multi-functional protein (MBP)-BSP-HAP mimicking natural bone formation was rationally designed and constructed to possess common features of NCPs, including binding calcium ions, binding collagen and binding hydroxyapatite. The present study shows that (MBP)-BSP-HAP can act as a templating analogue to bind collagen fibrils and regulate the growth behavior of hydroxyapatite. Bone-like highly organized hydroxyapatite becomes periodically arranged inside the collagen fibrils as (MBP)-BSP-HAP functions in synergy with polyacrylic acid. This work provides a promising method to realize collagen intrafibrillar mineralization by taking advantage of a rationally designed multi-functional protein based on functional domains of natural NCPs. It may shed light on bio-process-inspired approaches for more economic and efficient biomimetic synthesis, and it is also helpful in understanding the mysterious process of bone formation for bone regeneration and tissue repair.

Acknowledgements

This work was financially supported by the National Natural Science Foundation of China (51161140399), the Ministry of Science and Technology of China (L2015RR0040), and the Fundamental Research Funds for the Central Universities (WHUT, 2013-Ia-037 and 2013-YB-019).

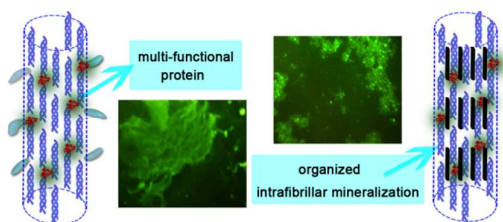
Notes and references

- State Key Laboratory of Advanced Technology for Materials Synthesis and Processing, Wuhan University of Technology, Wuhan, 430070, China. E-mail address: zyfu@whut.edu.cn
- School of Chemistry, Chemical Engineering, and Life Science, Wuhan University of Technology, Wuhan, 430070, China. E-mail address: h.xie@whut.edu.cn
- Laboratory of Inorganic Materials Chemistry, University of Namur, B-5000 Namur, Belgium
- Department of Materials Engineering, Monash University, Victoria 3800, Australia

† Electronic Supplementary Information (ESI) available: [details of any supplementary information available should be included here]. See DOI: 10.1039/b000000x/

- 1 S. Mann, D. D. Archibald, J. M. Didymus, T. Douglas, B. R. Heywood, F. C. Meldrum, N. J. Reeves, *Science* 1993, **261**, 1286-1292.
- 2 C. Sanchez, H. Arribart, M. M. G. Guille, *Nat. Mater.* 2005, **4**, 277-288.
- 3 F. Bouville, E. Maire, S. Meille, B. Van de Moortele, A. J. Stevenson, S. Deville, *Nat. Mater.* 2014, **13**, 508-514.
- 4 E. Munch, M. E. Launey, D. H. Alsem, E. Saiz, A. P. Tomsia, R. O. Ritchie, *Science* 2008, **322**, 1516-1520.
- 5 M. A. Meyers, J. McKittrick, P. Y. Chen, *Science* 2013, **339**, 773-779.
- 6 Y. M. Zheng, H. Bai, Z. B. Huang, X. L. Tian, F. Q. Nie, Y. Zhao, J. Zhai, L. Jiang, *Nature* 2010, **463**, 640-643.
- 7 K. S. Liu, L. Jiang, *Nano Today* 2011, **6**, 155-175.
- 8 I. Sethmann, *Science* 2013, **339**, 1281-1282.
- 9 F. Natalio, T. P. Corrales, M. Panthofer, D. Schollmeyer, I. Lieberwirth, W. E. Muller, M. Kappl, H. J. Butt, W. Tremel, *Science* 2013, **339**, 1298-1302.
- 10 C. Du, G. Falini, S. Fermani, C. Abbott, J. Moradian-Oldak, *Science* 2005, **307**, 1450-1454.
- 11 Q. Q. Hoang, F. Sicheri, A. J. Howard, D. S. C. Yang, *Nature* 2003, **425**, 977-980.
- 12 M. B. Dickerson, K. H. Sandhage, R. R. Naik, *Chem. Rev.* 2008, **108**, 4935-4978.
- 13 J. D. Currey, *Science* 2005, **309**, 253-254.
- 14 H. Peterlik, P. Roschger, K. Klaushofer, P. Fratzl, *Nat. Mater.* 2006, **5**, 52-55.
- 15 G. Mayer, *Science* 2005, **310**, 1144-1147.
- 16 A. K. Nair, A. Gautieri, S. W. Chang, M. J. Buehler, *Nat. Commun.* 2013, **4**, 1724-1732.
- 17 L. C. Palmer, C. J. Newcomb, S. R. Kaltz, E. D. Spoerke, S. I. Stupp, *Chem. Rev.* 2008, **108**, 4754-4783.
- 18 M. J. Olszta, X. Cheng, S. S. Jee, R. Kumar, Y.-Y. Kim, M. J. Kaufman, E. P. Douglas, L. B. Gower, *Mater. Sci. Eng. R.* 2007, **58**, 77-116.
- 19 A. George, A. Veis, *Chem. Rev.* 2008, **108**, 4670-4693.
- 20 S. Wang, X. Wen, A. DeVties, Y. Bagdagulyan, A. Morita, J. Golen, J. Duman, A. Rheingold, *J. Am. Chem. Soc.* 2014, **136**, 8973-8981.
- 21 S. Wang, X. Wen, P. Nikolovski, V. Juwita, J. Arifin, *Chem. Comm.* 2012, **48**, 11555-11557.
- 22 S. Boonrungsiman, E. Gentleman, R. Carzaniga, N. D. Evans, D. W. McComb, A. E. Porter, M. M. Stevens, *Proc. Natl. Acad. Sci. USA* 2012, **109**, 14170-14175.
- 23 F. Nudelman, A. J. Lausch, N. A. Sommerdijk, E. D. Sone, *J. Struct. Biol.* 2013, **183**, 258-269.
- 24 F. Nudelman, K. Pieterse, A. George, P. H. Bomans, H. Friedrich, L. J. Brylka, P. A. Hilbers, G. de With, N. A. Sommerdijk, *Nat. Mater.* 2010, **9**, 1004-1009.
- 25 A. S. Deshpande, E. Beniash, *Cryst. Growth Des.* 2008, **8**, 3084-3090.
- 26 L. B. Gower, *Chem. Rev.* 2008, **108**, 4551-4627.
- 27 Y. Y. Kim, N. B. J. Hetherington, E. H. Noel, R. Kroger, J. M. Charnock, H. K. Christenson, F. C. Meldrum, *Angew. Chem. Int. Ed.* 2011, **50**, 12572-12577.
- 28 A. S. Deshpande, P. A. Fang, X. Zhang, T. Jayaraman, C. Sfeir, E. Beniash, *Biomacromolecules* 2011, **12**, 2933-2945.
- 29 Y. Liu, Y. K. Kim, L. Dai, N. Li, S. O. Khan, D. H. Pashley, F. R. Tay, *Biomaterials* 2011, **32**, 1291-1300.
- 30 Y. Liu, N. Li, Y. P. Qi, L. Dai, T. E. Bryan, J. Mao, D. H. Pashley, F. R. Tay, *Adv. Mater.* 2011, **23**, 975-980.
- 31 L. Dai, Y. Qi, L. Niu, Y. Liu, C. Pucci, S. Looney, J. Ling, D. H. Pashley, F. R. Tay, *Cryst. Growth Des.* 2011, **11**, 3504-3511.
- 32 M. Wuttke, S. Muller, D. P. Nitsche, M. Paulsson, F. G. Hanisch, P. Maurer, *J. Biol. Chem.* 2001, **276**, 36839-36848.
- 33 G. S. Baht, G. K. Hunter, H. A. Goldberg, *Matrix Biol.* 2008, **27**, 600-608.
- 34 C. L. Chen, N. L. Rosi, *Angew. Chem. Int. Edit.* 2010, **49**, 1924-1942.
- 35 M. Sarikaya, C. Tamerler, A. K. Jen, K. Schulten, F. Baneyx, *Nat. Mater.* 2003, **2**, 577-585.
- 36 B. L. Adams, A. S. Finch, M. M. Hurley, D. A. Sarkes, D. N. Stratis-Cullum, *Adv. Mater.* 2013, **25**, 4585-4591.
- 37 M. Gungormus, H. Fong, I. W. Kim, J. S. Evans, C. Tamerler, M. Sarikaya, *Biomacromolecules* 2008, **9**, 966-973.
- 38 F. A. Quijoch, J. C. Spurlino, L. E. Rodseth, *Structure* 1997, **5**, 997-1015.
- 39 C. E. Tye, G. K. Hunter, H. A. Goldberg, *J. Biol. Chem.* 2005, **280**, 13487-13492.
- 40 S. E. Wolf, J. Leiterer, V. Pipich, R. Barrea, F. Emmerling, W. Tremel, *J. Am. Chem. Soc.* 2011, **133**, 12642-12649.
- 41 S. Weiner, P. A. Price, *Calcif. Tissue Int.* 1986, **39**, 365-375.
- 42 D. N. Zeiger, W. C. Miles, N. Eidelman, S. L. Gibson, *Langmuir* 2011, **27**, 8263-8268.
- 43 R. Fujisawa, Y. Nodasaka, Y. Kuboki, *Calcif. Tissue Int.* 1995, **56**, 140-144.
- 44 Y. Yang, Q. Cui, N. Sahai, *Langmuir* 2010, **26**, 9848-9859.

Table of contents entry



A multi-functional protein (MBP)-BSP-HAP is rationally designed to induce apatite periodically arranged inside collagen fibrils in synergy with polyacrylic acid.